

## Molecular Recognition-Induced Structural Flexibility in ZIF-71

*J. Farrando-Perez,<sup>1</sup> A. Missyul,<sup>2</sup> A. Martín-Calvo,<sup>3</sup> C. Abreu-Jauregui,<sup>1</sup> V. Ramírez-Cerezo,<sup>1,4</sup> L. Daemen,<sup>5</sup> Y.Q. Cheng,<sup>5</sup> A.J. Ramirez-Cuesta,<sup>5</sup> S. Calero,<sup>6</sup> C. Carrillo-Carrión,<sup>7</sup> J. Silvestre-Albero<sup>1,\*</sup>*

<sup>1</sup>Advanced Materials Laboratory, Department of Inorganic Chemistry-University Institute of Materials, University of Alicante, E-03690 San Vicente del Raspeig, Spain

<sup>2</sup>CELLS – ALBA Synchrotron, Cerdanyola del Vallés, Barcelona, Spain

<sup>3</sup>Center for Nanoscience and Sustainable Technologies (CNATS), Dpt. Physical, Chemical and Natural Systems, Universidad Pablo de Olavide, Seville, Spain

<sup>4</sup>Institut Laue-Langevin, 71 avenue des Martyrs, 38000, Grenoble, France

<sup>5</sup>Spallation Neutron Source, Oak Ridge National Laboratory, Oak Ridge, TN 37831, USA

<sup>6</sup>Department of Applied Physics, Eindhoven University of Technology, Eindhoven, The Netherlands

<sup>7</sup>Institute of Chemical Research (IIQ), CSIC – University of Seville, 41092 Seville, Spain

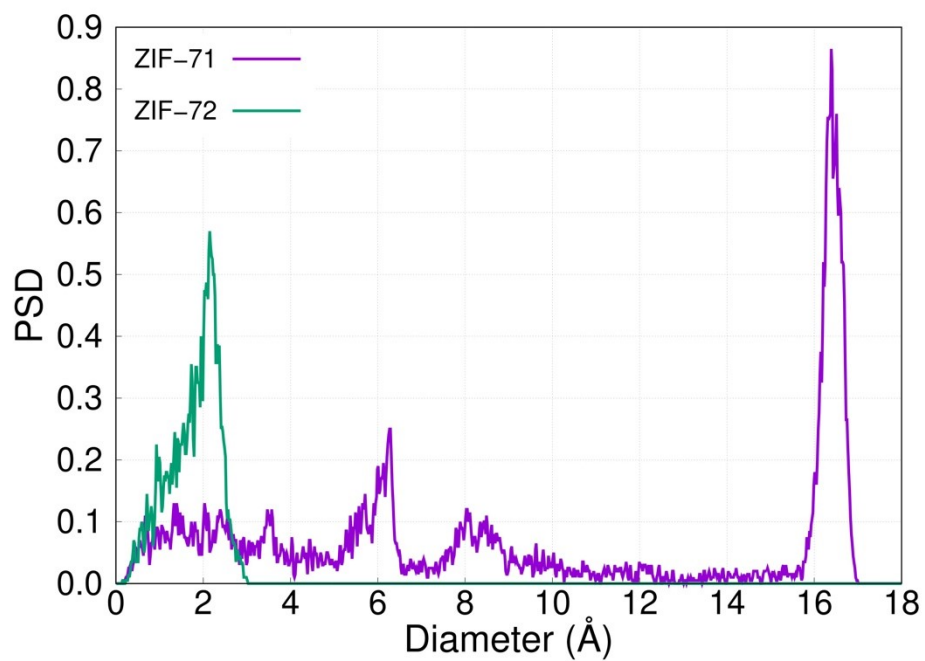
### SUPPORTING INFORMATION

Figures	Page
<b>Figure S1.</b> Simulated pore size distribution (PSD) for ZIF-71 and ZIF-72.	S3
<b>Figure S2.</b> Adsorption kinetic studies for (A) phenol and (B) chlorobenzene at 298 K in ZIF-71 sample.	S3
<b>Figure S3.</b> Simulated adsorption isotherms for phenol and chlorobenzene in ZIF-71 and ZIF-72.	S4
<b>Figure S4. A</b> Amplification of the OH and Cl distances in the two probes evaluated with the Cl groups in the ZIF-71 linker, and <b>B</b> Amplification of the intermolecular distances in equilibrium upon adsorption in ZIF-71.	S5
<b>Figure S5.</b> Immersion calorimetry measurements of ZIF-71 into (A) water, (B) a phenol/water solution, and (C) a chlorobenzene/water solution.	S6
<b>Figure S6.</b> Adsorption kinetic studies for (A) phenol and (B) chlorobenzene at 298 K in ZIF-71 sample under acidic conditions (pH 3.5 adjusted using a HCl solution). Average adsorption kinetics (data from Figure S2), obtained under non-modified pH conditions, have been added as a grey slashed line for the sake of comparison.	S7
<b>Figure S7.</b> Synchrotron X-ray powder diffraction patterns of ZIF-71 before and after the chlorobenzene and phenol adsorption tests under acidic	S7

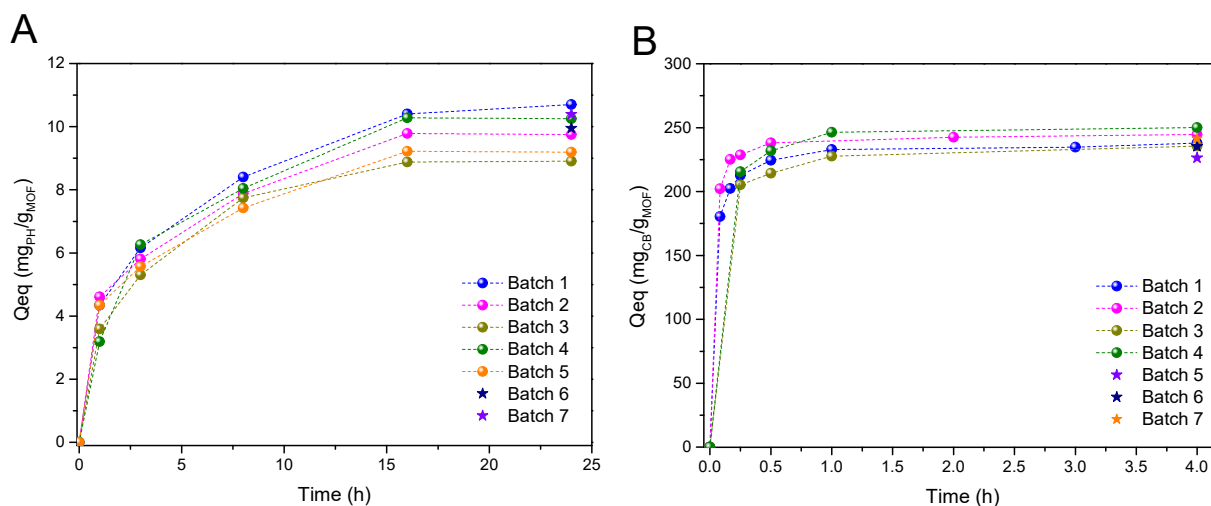
conditions (beam energy 20 keV).	
<b>Figure S8.</b> Synchrotron X-ray powder diffraction patterns of ZIF-71 before and after the phenol adsorption tests (beam energy 30 keV). The used sample was submitted to a thermal treatment at 453 K to promote the phase transition. Low 2 Theta peaks in ZIF-71@phenol (ca. 1.2°) correspond to entrapped water.	S8
<b>Figure S9.</b> Synchrotron X-ray powder diffraction patterns of ZIF-71 before and after the chlorobenzene adsorption tests (beam energy 17.5 keV). The used sample was submitted to a thermal treatment at 453 K to promote the phase transition.	S9
<b>Figure S10.</b> Representative FESEM images of ZIF-71 after the phenol adsorption process, a subsequent drying and a heat treatment at 453 K.	S9
<b>Figure S11.</b> Synchrotron X-ray powder diffraction patterns of ZIF-71 before and after exposure to the vapors of an aqueous solution of phenol (50 ppm) (beam energy 20 keV).	S10
<b>Figure S12.</b> Rietveld refinement of the different SXRPD patterns obtained.	S11

Tables	Page
<b>Table S1:</b> Lennard-Jones parameters and partial charges of the atoms from the structures. Different types of atoms were defined for a given element according to their chemical environment. The proposed labelling of atoms is shown below.	S12
<b>Table S2.</b> Henry coefficients and Heat of adsorption for the three probes evaluated obtained from the GCMC simulations.	S12- S13
<b>Table S3:</b> Structural parameters calculated for ZIF-71 before (pristine) and after being applied in the phenol and chlorobenzene adsorption process. The amount of ZIF-72 determined from the Rietveld refinement is included for each specific case.	S13

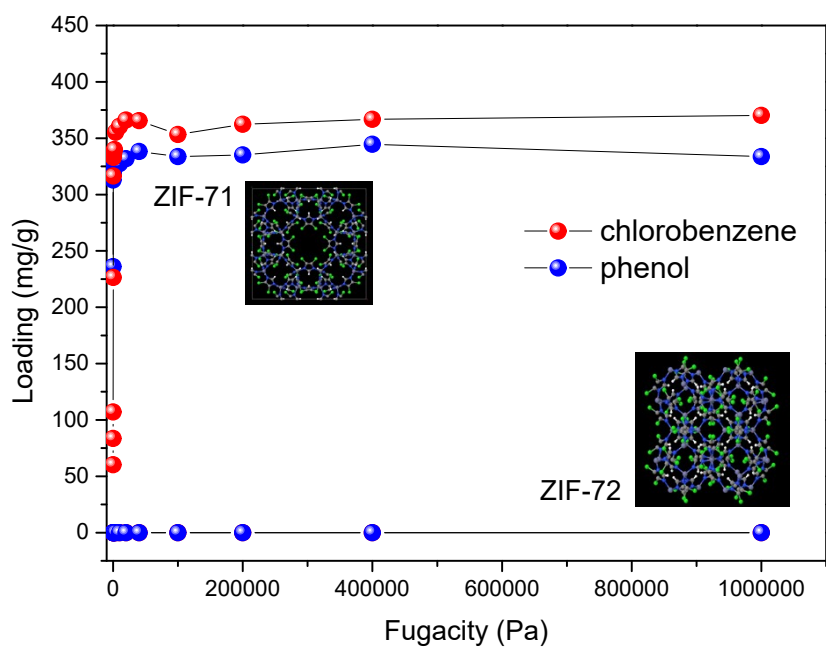
## FIGURES



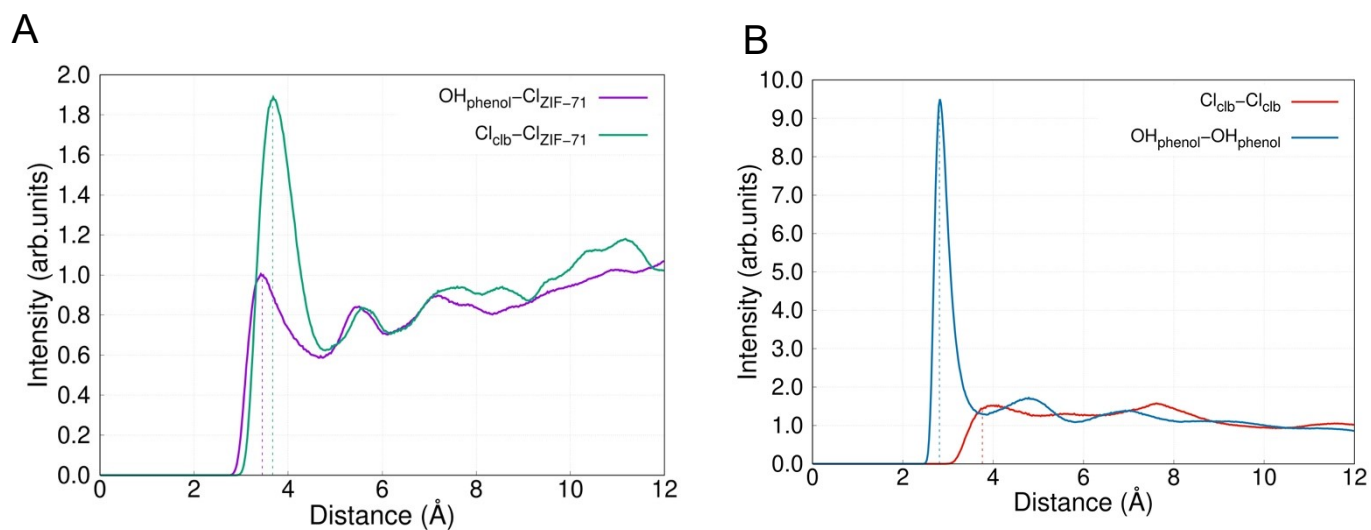
**Figure S1.** Simulated pore size distribution (PSD) for ZIF-71 and ZIF-72.



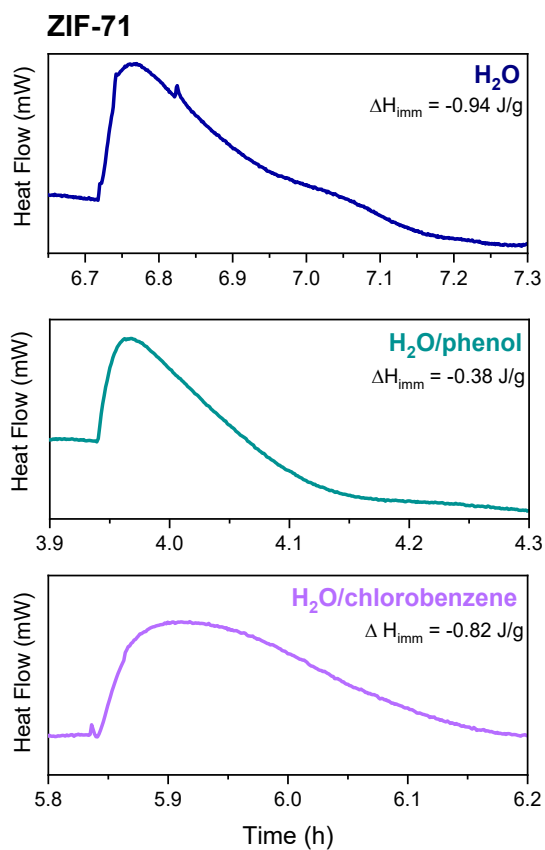
**Figure S2.** Adsorption kinetic studies for (A) phenol and (B) chlorobenzene at 298 K in ZIF-71 sample.



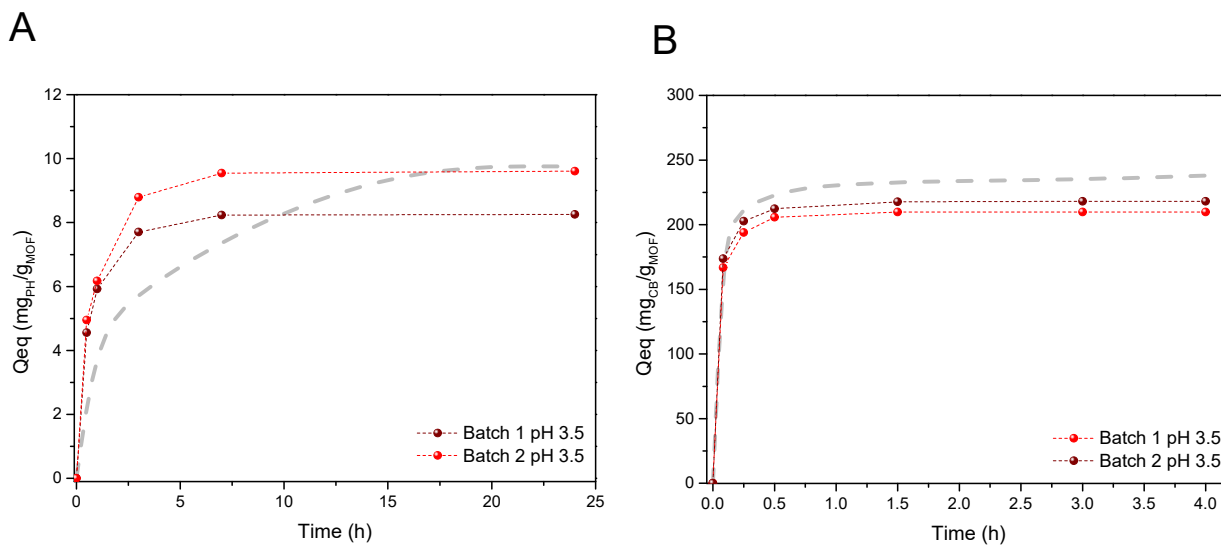
**Figure S3.** Simulated adsorption isotherms for phenol and chlorobenzene in ZIF-71 and ZIF-72.



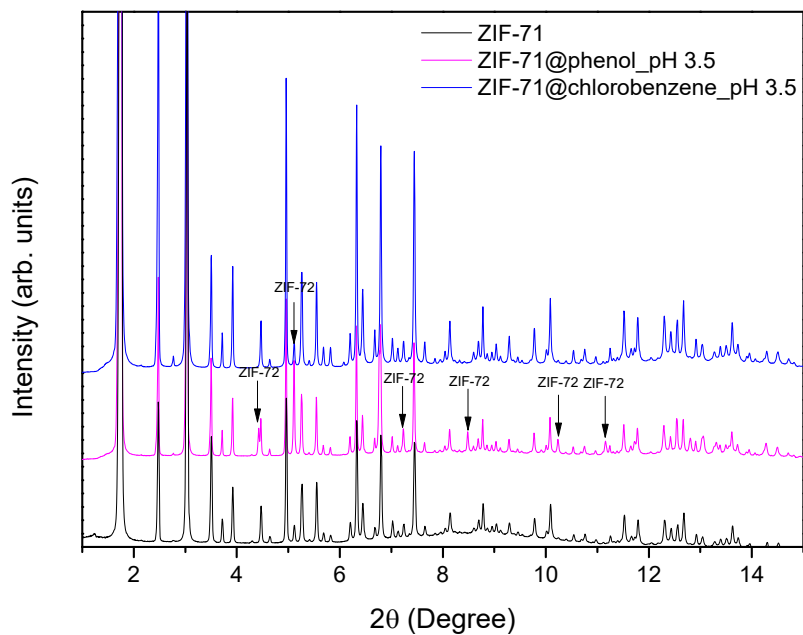
**Figure S4.** **A** Amplification of the OH and Cl distances in the two probes evaluated with the Cl groups in the ZIF-71 linker, and **B** Amplification of the intermolecular distances in equilibrium upon adsorption in ZIF-71.



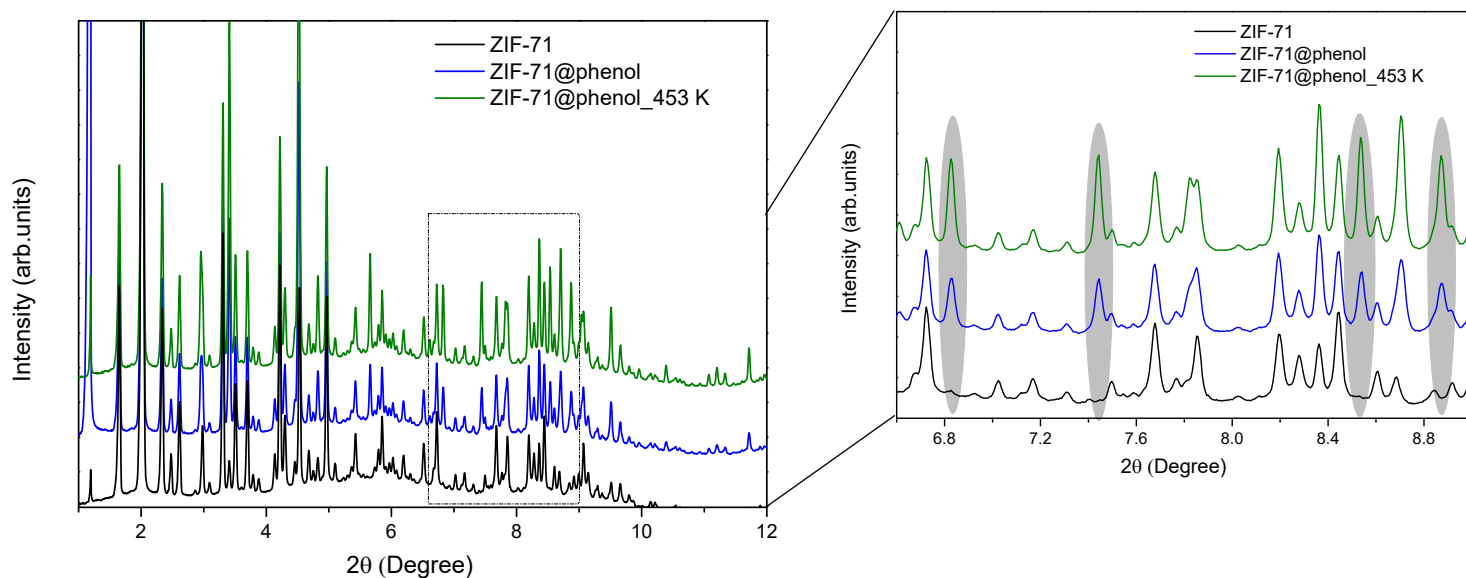
**Figure S5.** Immersion calorimetry measurements of ZIF-71 into (A) water, (B) a phenol/water solution, and (C) a chlorobenzene/water solution.



**Figure S6.** Adsorption kinetic studies for (A) phenol and (B) chlorobenzene at 298 K in ZIF-71 sample under acidic conditions (pH 3.5 adjusted using a HCl solution). Average adsorption kinetics (data from Figure S2), obtained under non-modified pH conditions, have been added as a grey slashed line for the sake of comparison.

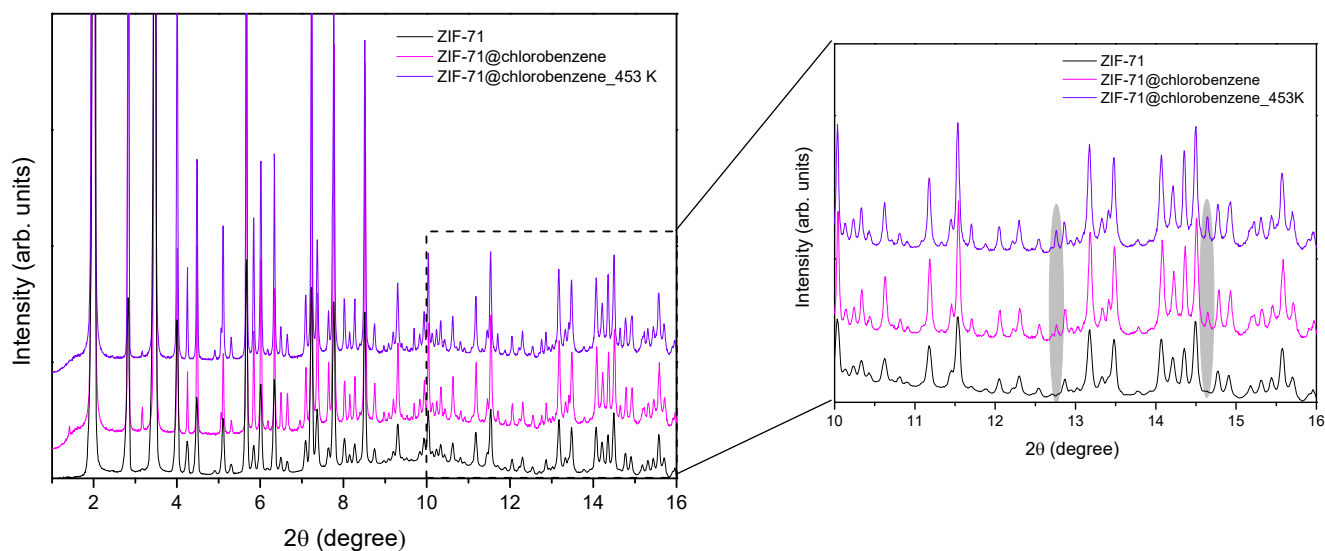


**Figure S7.** Synchrotron X-ray powder diffraction patterns of ZIF-71 before and after the chlorobenzene and phenol adsorption tests under acidic conditions (beam energy 20 keV).

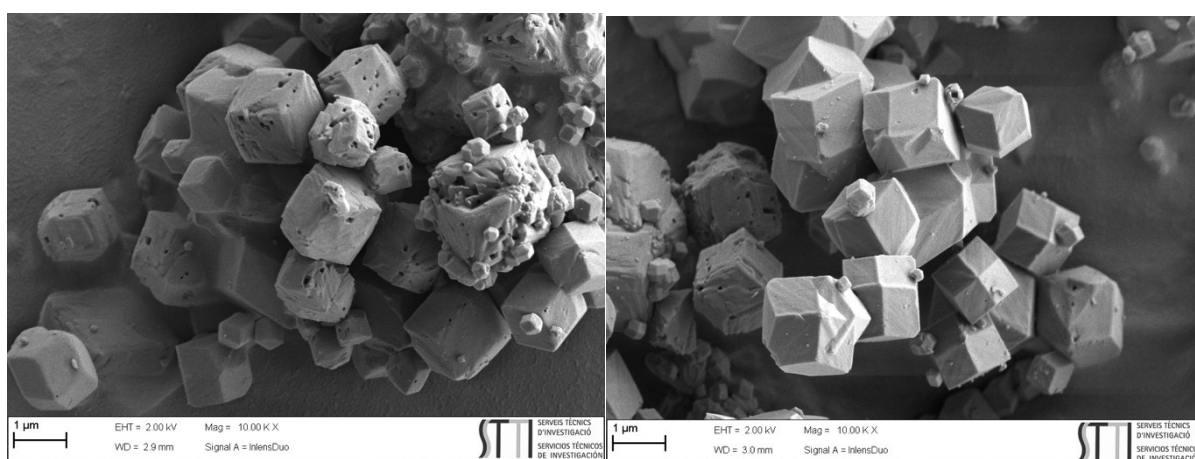


**Figure S8.** Synchrotron X-ray powder diffraction patterns of ZIF-71 before and after the phenol adsorption tests (beam energy 30 keV). The used sample was submitted to a thermal treatment at 453 K to promote the phase transition. Low 2 Theta peaks in ZIF-71@phenol (ca.  $1.2^\circ$ ) correspond to entrapped water.

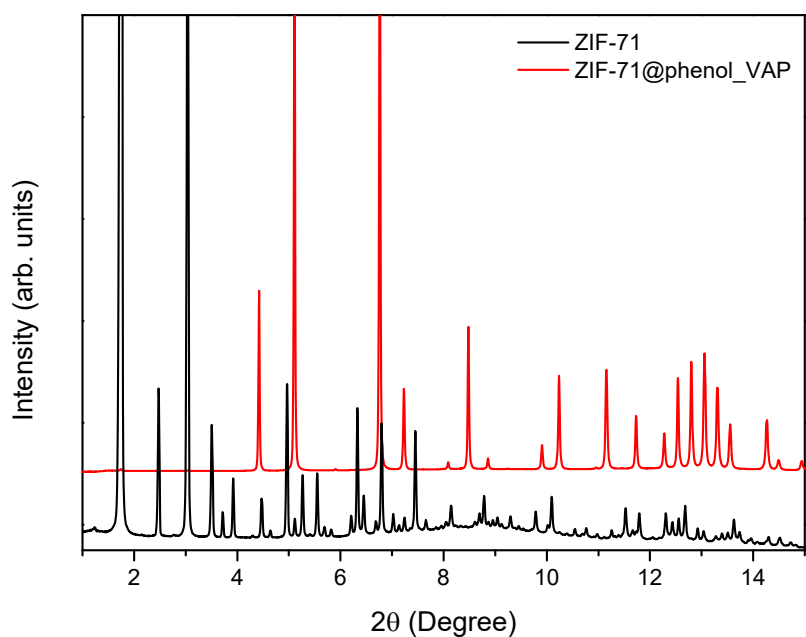




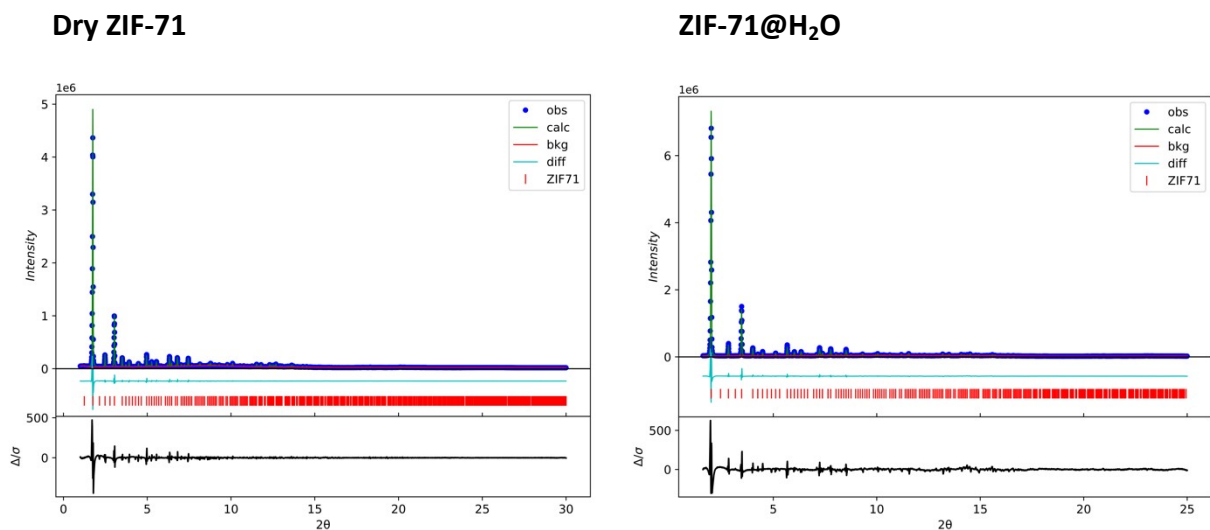
**Figure S9.** Synchrotron X-ray powder diffraction patterns of ZIF-71 before and after the chlorobenzene adsorption tests (beam energy 17.5 keV). The used sample was submitted to a thermal treatment at 453 K to promote the phase transition.



**Figure S10.** Representative FESEM images of ZIF-71 after the phenol adsorption process, a subsequent drying and a heat treatment at 453 K.



**Figure S11.** Synchrotron X-ray powder diffraction patterns of ZIF-71 before and after exposure to the vapors of an aqueous solution of phenol (50 ppm) (beam energy 20 keV).



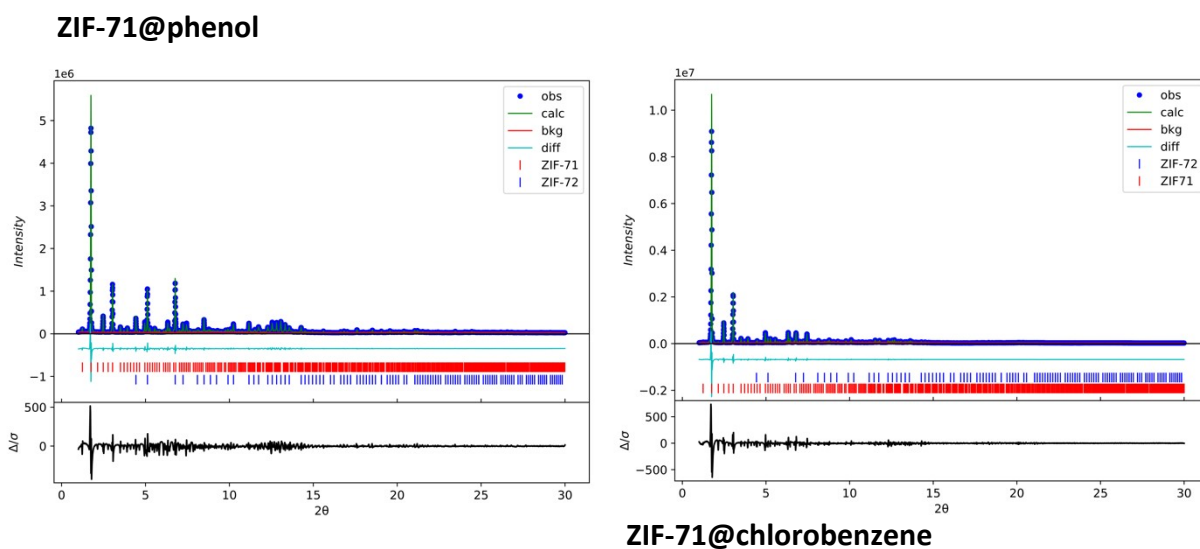


**Figure S12.** Rietveld refinement of the different SXRPD patterns obtained.

## TABLES

**Table S1:** Lennard-Jones parameters and partial charges of the atoms from the structures. Different types of atoms were defined for a given element according to their chemical environment. The proposed labelling of atoms is shown below.

Atom Type	$\epsilon/k_B$ (K)	$\sigma$ (Å)	charge ( $e^-$ )
Zn1	62.40	2.462	0.7

C1	52.84	3.431	0.0371
H1	22.14	2.571	0.049
N2	34.72	3.261	-0.19355
C3	52.84	3.431	0.0189
Cl4	114.23	3.517	-0.0434

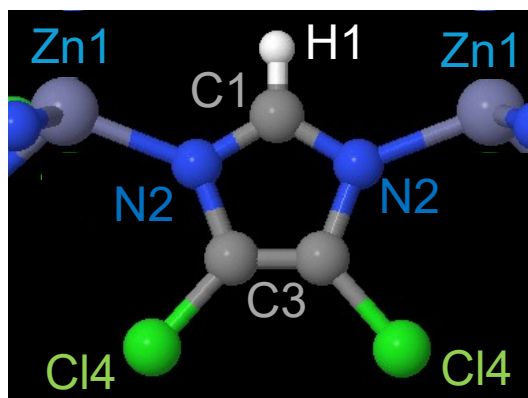


**Table S2.** Henry coefficients and Heat of adsorption for the three probes evaluated obtained from the GCMC simulations.

Henry Coefficient (ml/kg/Pa)					
ZIF-71			ZIF-72		
phenol	chlorobenzene	water	phenol	chlorobenzene	water
$1.10 \pm 0.01$	$0.135 \pm 0.001$	$1.1 \cdot 10^{-6} \pm 9.6 \cdot 10^{-9}$	$1.0 \cdot 10^{-95} \pm 4 \cdot 10^{-95}$	$1.1 \cdot 10^{-142} \pm 4.6 \cdot 10^{-142}$	$1.2 \cdot 10^{-9} \pm 2 \cdot 10^{-11}$

Heat of Adsorption (kJ/mol)					
ZIF-71			ZIF-72		
phenol	chlorobenzene	water	phenol	chlorobenzene	water
$-66.63 \pm 0.11$	$-61.49 \pm 0.70$	$-13.89 \pm 0.10$	$491 \pm 30$	$780 \pm 57$	$-6.72 \pm 0.06$

**Table S3:** Structural parameters calculated for ZIF-71 before (pristine) and after being applied in the phenol and chlorobenzene adsorption process. The amount of ZIF-72 determined from the Rietveld refinement is included for each specific case.

Sample	ZIF-71		ZIF-72	
	a, Å	wt.%%	a, Å	wt.%%
ZIF-71 dry	28.6387	100%	Not observed	
ZIF-71@phenol	28.6428	46.5	19.6513	53.5
ZIF-71@chlorobenzene	28.6304	100%	Not observed	